[CANCER RESEARCH 62, 1420–1424, March 1, 2002]

Subcellular Localization of NAD(P)H:quinone Oxidoreductase 1 in Human Cancer Cells[1]

Shannon L. Winski, Yiannis Koutalos, David L. Bentley, and David Ross[2]

Departments of Pharmaceutical Sciences [S. L. W., D. R.] and Physiology and Biophysics [Y. K.], University of Colorado Health Sciences Center, Denver, Colorado 80017, and Imaging Facility, University of Arizona, Tucson, Arizona 85721 [D. L. B.]

ABSTRACT

NAD(P)H:quinone oxidoreductase 1 (NQO1) is implicated in both chemoprevention and bioactivation of DNA-damaging antitumor agents. NQO1 is mainly cytosolic, but distribution in other cellular compartments, particularly in tumor cells, is poorly defined. Nuclear NQO1 in HT29 human colon carcinoma and H661 human non-small cell lung cancer cells was observed using both confocal microscopy and immunoelectron microscopy. NQO1 was not detected in mitochondria, golgi, or endoplasmic reticulum. In addition, purified intact nuclei from HT29 cells contained immunoreactive NQO1, which was catalytically active as determined by conventional activity assay. In summary, we have confirmed the presence of nuclear NQO1, which has implications for chemoprotection and bioactivation of DNA-damaging antitumor agents.

INTRODUCTION

NQO1[3] (EC 1.6.99.2) or DT-diaphorase is an obligate two-electron reductase, which acts as a chemoprotectant by catalyzing the reduction and detoxification of a broad range of quinone substrates (1, 2). NQO1 also plays a role as an antioxidant enzyme and generates antioxidant forms of ubiquinone and α-tocopherol (3–5). Paradoxically, NQO1 also catalyzes the bioactivation of antitumor quinones, which exert their toxicity through direct DNA damage (6, 7). This is currently under consideration as a therapeutic strategy to exploit the elevated NQO1 activity found in certain human tumors.

The enzyme is polymorphic in humans with a homozygous C609T point mutation ranging from 4 to 22%, depending on ethnicity (8). The homozygous C609T variant results in a null phenotype because of the loss of protein via rapid polyubiquitination and proteosomal degradation (9). The presence of this C609T mutation has allowed for extensive epidemiological studies on the importance of NQO1 in a variety of disease states. Lack of NQO1 activity has been associated with an increased incidence of benzene-induced hemotoxicity (10), chemotherapy-related myeloid malignancies (11), leukemias (12), and basal cell carcinoma (13).

NQO1 is found in a variety of human tissues throughout the body in particular in epithelial and endothelial cells. In addition to normal tissues, NQO1 is overexpressed in a variety of solid tumors, including thyroid, adrenal, breast, ovarian, colon, cornea, and lung (14–16). There is little known about the subcellular localization of NQO1 in human tissues. In this study, we demonstrate the presence of NQO1 in the nucleus, which may have important implications for both chemoprotection and the bioactivation of DNA-damaging antitumor quinones.

Received 8/28/01; accepted 1/3/02.

The costs of publication of this article were defrayed in part by the payment of page charges. This article must therefore be hereby marked *advertisement* in accordance with 18 U.S.C. Section 1734 solely to indicate this fact.

[1] Supported by NIH Grants R01 CA 51520 (to D. R.) and CA 79446 (to S. L. W.).

[2] To whom requests for reprints should be addressed, at Departments of Pharmaceutical Sciences, University of Colorado Health Sciences Center, Denver, CO 80017.

[3] The abbreviations used are: NQO1, NAD(P)H:quinone oxidoreductase 1; DCPIP, 2,6-dichlorophenol-indophenol.

MATERIALS AND METHODS

Materials. Cell culture medium was obtained from Life Technologies, Inc. (Gaithersburg, MD), and fetal bovine serum was from Gemini BioProducts, Inc. (Calabasas, CA). Other cell culture materials were purchased from Fisher Scientific (Pittsburgh, PA). Mouse antihuman NQO1 primary antibody from hybridoma clone A180 was maintained by University of Colorado core facilities and does not cross-react with other souces of NQO1. Peroxidase-conjugated goat antimouse was obtained from Jackson ImmunoResearch Laboratories (Bar Harbor, ME). Secondary and tertiary antibodies for immunoelectron microscopy (biotinylated goat antimouse and 10 nm of gold-conjugated antibiotin, respectively) were obtained from BBInternational (Vector Labs, Burlingame, CA). Antilamin B1 antibody was obtained from Zymed Laboratories, Inc. (San Francisco, CA). All chemicals for electron microscopy were obtained from Polysciences, Inc. (Warrington, PA). Precast 12% acrylamide gels were purchased from Bio-Rad (Hercules, CA). Immobilon-P Western blotting membrane, antiactin monoclonal antibody, DCPIP, and all other chemicals were purchased from Sigma Chemical Co. (St. Louis, MO). H661 human non-small cell lung carcinoma and HT29 human colon carcinoma cells were obtained from American Type Culture Collection and maintained at 37°C under a humidified atmosphere with 5% CO_2. Cells were grown as monolayers in RPMI 1640 supplemented with 20% fetal bovine serum, 2 mM L-glutamine, 100 units/ml penicillin, and 100 μg/ml streptomycin and were *Mycoplasma* free.

Isolation and Analysis of Intact Nuclei. Freshly collected cells were washed three times in PBS and resuspended in 0.25 M sucrose containing 10 mM triethanolamine and 10 mM acetic acid (pH 7.6), then homogenized until 90% of the cells were lysed (monitored by trypan blue exclusion). All steps of the purification process were carried out at 4°C. The homogenate was centrifuged at 600 $\times$ *g* for 10 min to pellet nuclei, which were further purified on a sucrose gradient (60% barrier). The supernatant was centrifuged at 100,000 $\times$ *g* for 60 min to isolate cytosol. Nuclei were washed in 150 mM Tris-HCl (pH 8), then disrupted by sonication. Protein samples were electrophoresed on 12% agarose, 0.1% SDS, before transfer to Immobilon P membrane (5 μg of total protein loaded each lane). Purity of subcellular compartments was monitored by immunoblot analysis using antibodies against actin for cytosol and lamin B1 for nuclei. Activity of NQO1 was measured as the dicoumarol-inhibitable fraction of DCPIP reduction as described (1) with modifications (17) and normalized to total nuclear or cytosolic protein (Bio-Rad).

Confocal Microscopy. Cells were grown on glass coverslips and fixed with 4% formaldehyde and 0.1% glutaraldehyde in PBS. Confocal images were acquired with a 100 $\times$ oil immersion lens (numerical aperture = 1.3) on a Zeiss Axiovert 135 microscope equipped with a CARV optical module ("spinning disc confocal") and a Hamamatsu Orca (C4742–95) digital camera (6.7 $\times$ 6.7 μm of physical pixels). The *Z*-axis resolution was 0.45 μm. The enzyme distribution was confirmed in confocal images obtained through a digital deconvolution process. For these images, the system used was comprised of an Olympus IX70-inverted microscope with a 100 $\times$ oil immersion lens (numerical aperture = 1.35), a Photometrics PXL camera with Kodak KAF1400 chip (6.7 $\times$ 6.7 μm of physical pixels), and a Silicon Graphics O2 computer with DeltaVision deconvolution software (Applied Precision, Seattle, WA). The step size for the sectioning was 0.2 μm for the deconvolved images. For nuclear staining with Hoechst 33342, 4′,6-diamidino-2-phenylindole excitation and emission filters were used, 360 and 457 nm, respectively. Texas red fluorescence was measured with 555-nm excitation and 617-nm emission. Intensity profiles were generated through image analysis with the use of NIH Image, version 1.62.

Immunoelectron Microscopy. HT29 cells were harvested by trypsinizing and fixed through ultrarapid freezing before embedding and microwave im-

munolabeling. For cryofixation and freeze substitution, the cells were placed between copper Panama hats (Research Manufacturing Corp.) with slot grids as spacers. Both hats were pretreated with 0.1% lecithin and dried. The sample was rapidly frozen with a propane jet freezer at −160°C and 60 psi (Research Manufacturing Corp.; model MF 7200). The hats were broken apart in microfuge tubes filled with anhydrous acetone containing 0.2% glutaraldehyde and 0.1% uranyl acetate, which was precooled to −80°C. The samples were allowed to undergo freeze substitution for 12 h at this temperature, then warmed to −20°C. Acetone was removed, and the samples were washed twice with fresh methanol (−20°C). The sample was then infiltrated with 50% methanol/50% Unicryl resin followed by three changes in 100% resin. Blocks were hardened and cured under UV light at −20°C. Thin sections (70 nm) were cut on a MT 7000 microtome and placed on nickel grids. Unstained sections were labeled using microwave-controlled heating. A 35-μl sample was placed on a Teflon sheet, and a temperature probe was placed in a center dummy drop. Grids were placed on equivalent drops, and all binding steps were carried out at 37°C. Samples were blocked in 0.2% Tween 20 in PBS for 2.5 min followed by 4 × concentrated primary antibody for 2.5 min (monoclonal mouse antihuman NQO1 hybridoma supernatant). Samples were rinsed extensively in PBS followed by labeling with secondary antibody (biotinylated goat antimouse), rinsing in PBS, labeling with tertiary marker antibody (10 nM Gold-conjugated goat antibiotin), and rinsing in PBS. The antibody complex was fixed at room temperature in 4% formaldehyde/1% glutaraldehyde for 2.5 min followed by extensive rinsing in distilled water. After immunolabeling, samples were microwave counterstained at 60°C with saturated uranyl acetate and lead citrate for 1 min each stain. Negative controls included sections incubated without primary antibody. Sections were examined on a JEOL 100 CX II electron microscope at an accelerating voltage of 80 keV.

RESULTS

Confocal Microscopy. Using two-dimensional confocal microscopy ("spinning disc"), the intracellular distribution of NQO1 was visualized in HT29 and H661 cells (Fig. 1). The confocal images were obtained after focusing on the nucleus, which was visualized through staining with Hoechst 33342 stain (*green*), and NOQ1 was localized through visualization of Texas red-conjugated secondary antibody (*red*). In both HT29 and H661 cells, staining for NQO1 was observed throughout the cell. Its location within the nucleus is shown by yellow in overlay images, and the relative level of staining is depicted in the intensity profile generated by image analysis. In HT29 cells, NQO1 was primarily located in the cytoplasm with detectable but diminished levels in the nucleus. In H661, the contrast between nuclear and cytoplasmic levels was much less pronounced, indicating a higher nuclear:cytoplasmic ratio of NQO1 in these cells. Plotting the intensity profile of NQO1 staining in these cells supports these conclusions (Fig. 1). The enzyme distribution was confirmed separately by confocal images obtained through a digital deconvolution process (Fig. 2). The relative distribution of the enzyme in the nucleus and cytosol of HT29 and H661 cells was found to be similar with both approaches.

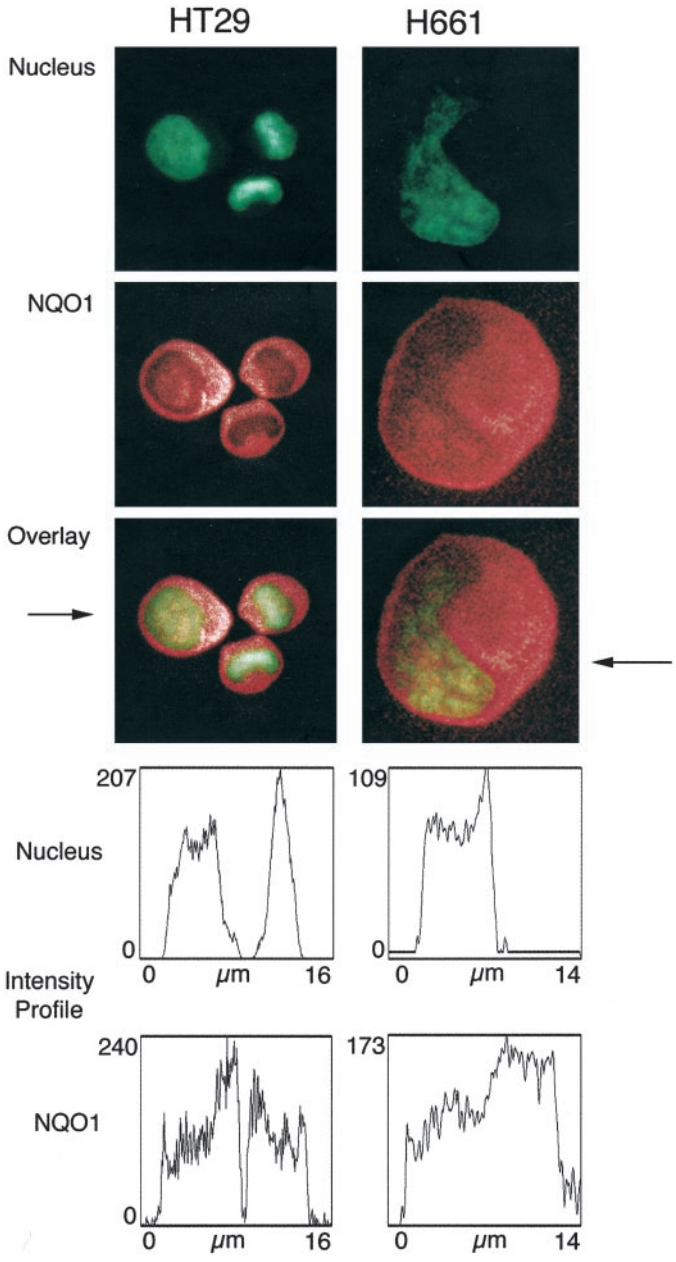

Fig. 1. Visualization of NQO1 in H661 non-small cell lung cancer and HT29 human colon carcinoma by spinning disc confocal microscopy. Cells were fixed on glass coverslips and labeled with Hoechst 33342 to stain nuclei (*green*) and Texas red-conjugated secondary antibody to anti-NQO1 primary antibody (*red*). *Overlay panels*, the colocalization of NQO1 in the nucleus (*yellow*). The relative levels of NQO1 and nuclear staining are presented as intensity profiles from computer-aided image analysis and given in relative fluorescence intensity units. Profiles were generated from *left* to *right* through the center of the *top left* cell (*arrow*) for HT29 cells and through the *center* of the H661 cell (*arrow*). *X* axis is distance (μm), and the *Y* axis is relative fluorescence units (linear scale).

Immunoelectron Microscopy. To confirm the results obtained by confocal microscopy and extend these observations, HT29 cells were analyzed using immunoelectron microscopy (Fig. 3), a technique with greater resolving power than light microscopy. The cells were subjected to cryopreservation through rapid freezing, followed by freeze substitution. Preparing cells in this manner ensures the preservation of the basal state of the cell, and minimal movement occurs through subcellular compartments (18). Immunoreactive NQO1 was visualized by the presence of 10 nM gold-conjugated goat antibiotin antibody in turn complexed with biotinylated goat antimouse and monoclonal mouse antihuman NQO1 (*arrowheads*). Immunogold labeling of NQO1 was observed clearly in the nucleus (*n*) and cytoplasm (*c*) but not mitochondria (*m*) of HT29 cells (Fig. 3*A*). To demonstrate relative labeling in the cell, the photomicrograph was scanned, and a cartoon of the cell was prepared with beads identified in yellow on a blue background representative of the cell (Fig. 3*B*). There was no apparent labeling of mitochondria (*m*), golgi apparatus (*g*), and endoplasmic reticulum (data not shown). There was no significant labeling of sections in the absence of primary antibody (Fig. 3, *B* and *D*).

NQO1 Protein in Isolated Nuclei. To confirm the nuclear localization of NQO1, nuclei from HT29 cells were isolated by differential centrifugation and purified through a sucrose gradient. Analysis of the protein by immunoblot clearly demonstrates the presence of NQO1 in the cytosol and nucleus of HT29 cells (Fig. 4). Purity of the isolated nuclear fraction was determined using actin as a cytosolic marker and

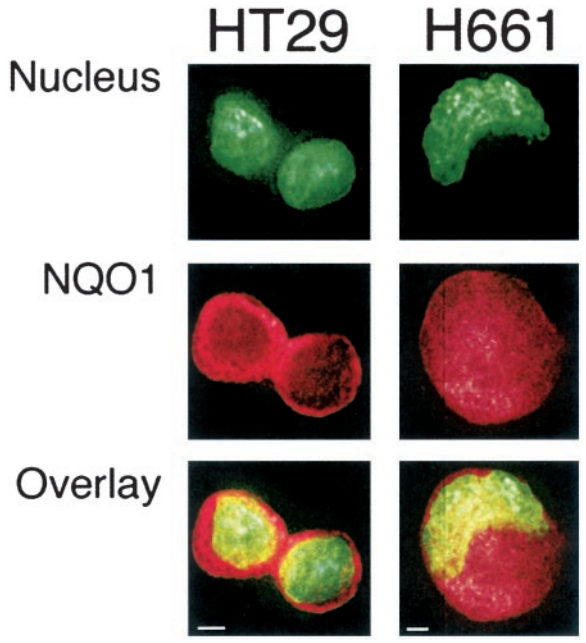

Fig. 2. Visualization of NQO1 in H661 non-small cell lung cancer cells and HT29 human colon carcinoma cells by digital deconvolution confocal microscopy. Cells were fixed on glass coverslips and labeled with Hoechst 33342 to stain nuclei (*green*) and Texas red-conjugated secondary antibody to anti-NQO1 primary antibody (*red*). *Overlay panels,* the colocalization of NQO1 in the nucleus (*yellow*). *Scale lines,* 2 μm.

lamin B1 as a nuclear marker. There was no significant presence of cytosol in the isolated nuclear fraction, indicating that NQO1 present in this sample originated from the nuclear compartment. To determine whether the protein was enzymatically active, the ability to reduce DCPIP was measured in the presence and absence of dicoumarol. Enzymatic activity was measured in both fractions but at a much higher level in cytosol (1613 $\pm$ 44 nmol of DCPIP reduced/min $\times$ mg of total cytosolic protein) compared with nucleus (36 $\pm$ 16 nmol of DCPIP reduced/min $\times$ mg of total nuclear protein).

DISCUSSION

There is little known about the subcellular distribution of NQO1 in human cells, and there is no definitive information on the presence or absence of nuclear NQO1. From studies in rat liver, the bulk of NQO1 (>84%) is located in the cytoplasm (19, 20). Lesser amounts were found in mitochondria (13%) and trace levels in golgi (1%) and microsomes (2%; Ref. 20). Although human and rat NQO1 have overlapping substrate specificities and share 85% amino acid homology, there are significant differences in post-translational processing that could affect the cellular distribution. Distribution in pig corpus luteum was similar to rat with NQO1

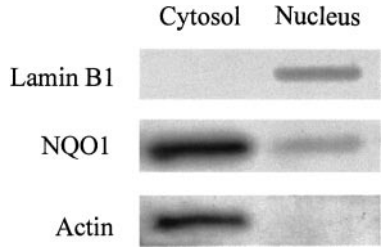

Fig. 4. Immunoblot analysis of protein from purified intact nuclei and cytosol isolated by cellular fractionation from HT29 (5 μg of total protein loaded each *lane*). Nuclear and cytosolic purity was confirmed by detection of the presence of marker proteins lamin B1 and actin for nucleus and cytosol, respectively.

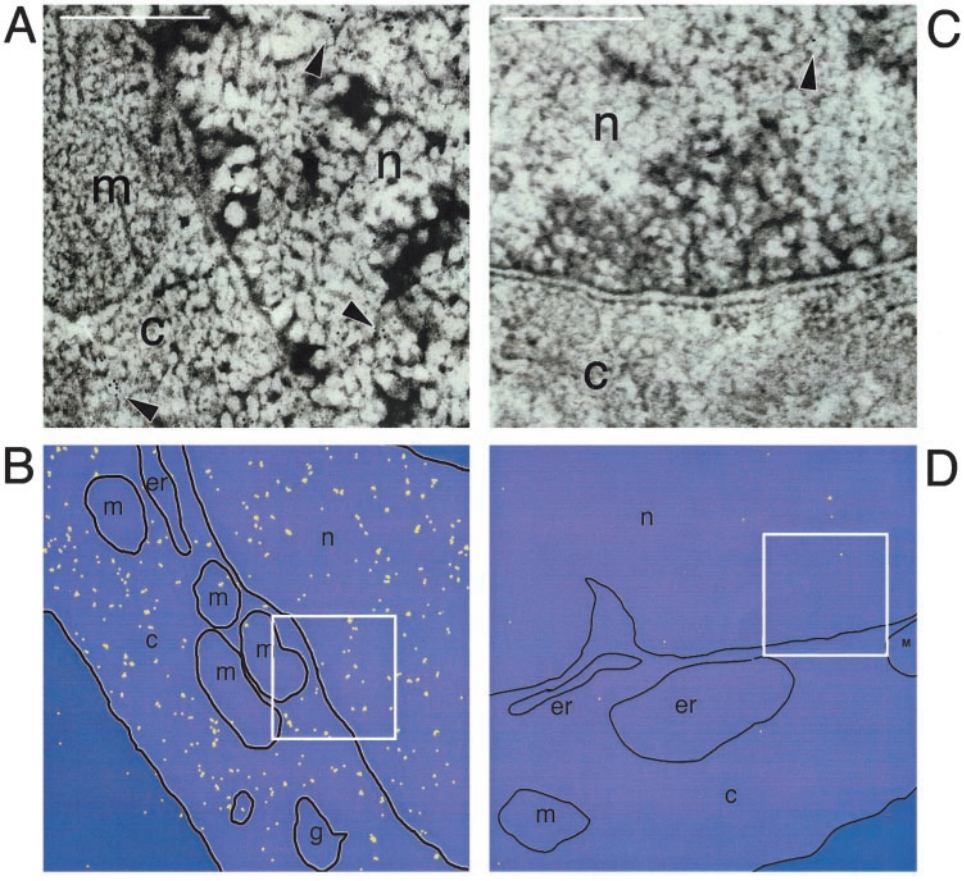

Fig. 3. Immunoelectron microscopic analysis of HT29 human colon carcinoma cells after cryopreservation and freeze substitution. NQO1 is visualized from a ternary complex of mouse anti-NQO1/biotinylated goat antimouse and 10-nm conjugated mouse antibiotin. *A,* recognition of NQO1 in HT29 cells demonstrated by the presence of 10-nm gold beads (*arrowheads*). NQO1 was localized to the nucleus (*n*) and cytosol (*c*) but does not occur in significant quantities in mitochondria (*m*) or golgi (*g*; scale line = 0.5 μm). In *C,* negative control samples were prepared by removing primary antibody in the sample preparation. In control samples, immunolabeling was scarce, and little nonspecific labeling was observed (scale line = 0.5 μm). To demonstrate relative labeling in the cell, the above photomicrographs were scanned, and a cartoon of the cell was prepared with beads identified in *yellow* on a *blue* background representative of the cell (*B,* positive staining; *D,* negative control; *box,* overlapping area in matching panels).

activity localized in cytoplasm, mitochondria, and microsomes (21). The above data were obtained by measuring enzymatic activity in subcellular fractions after differential centrifugation. Under these conditions, it is possible for soluble components to diffuse into or out of cellular compartments. To address this, microscopy can be used to visualize organelles of interest within a more fixed environment. We report here the subcellular distribution of NQO1 in human cancer cells and confirm the presence of this enzyme in the nucleus of HT29 and H661 cells. The data were obtained through a variety of sources, all of which indicate the presence of karyophilic NQO1. NQO1 was colocalized in the nucleus of H661 and HT29 cells visualized by confocal microscopy with dual labeling of the nucleus with Hoechst 33342 stain and immunolabeling of NQO1 with Texas red-conjugated antibody complex. Digital deconvolution confocal images were also obtained to confirm these results and demonstrated similar enzyme distributions. Activity assays and immunoblots also confirmed the presence of nuclear NQO1, although it is difficult to directly compare on a quantitative basis data obtained by microscopy and enzyme assay. All techniques used, however, demonstrated the presence of a significant nuclear pool of NQO1.

To extend these results, HT29 cells were analyzed by immunoelecron microscopy after ultrarapid cryopreservation and freeze substitution. Under these conditions, cellular components do not have an opportunity for movement, and cellular localization can be identified more readily (18). Using this technique, NQO1 was found in the nucleus and cytosol of HT29 cells, but no NQO1 labeling occurred in the golgi apparatus, endoplasmic reticulum, or mitochondria. Many sources report the presence of NQO1 in the mitochondria in a variety of species, including rat, pig, and human (19, 20, 22). Although the images obtained through immunoelectron microscopy do not support the presence of NQO1 in the mitochondria, it is possible that the loss of antigenicity that occurs when embedding cells in resin could account for the lack of positive labeling. However, it should not be discounted that mitochondrial localization observed in previous studies could be attributable to movement of NQO1 into this compartment in response to the stress of cell fractionation techniques.

Localization of proteins in the nucleus can occur through passive diffusion through nuclear pore complexes, active transport by nuclear localization signals, or binding to chaperone proteins. For efficient passive diffusion through the nuclear pore, a protein should be less than 40–60 kDa in size and, more importantly, <10 nm in diameter (23). NQO1 has a molecular mass of 61 kDa (two monomers of 30.7 kDa each), but analysis of the crystal structure (Protein Data Bank accession no. 1D4A) with Insight II software (Molecular Simulations, Inc.) indicates that NQO1 is relatively spherical with a diameter between 60 and 70 nm, depending on axis, making passive diffusion of even the monomeric form of NQO1 unlikely. The classic nuclear localization signal was identified from the sequence of large T antigen and consists of a consensus sequence, which is not present in the sequence of NQO1. NQO1 does, however, have two hsp70 binding sites (amino acids 4–15 and 245–266), and hsp70 is known to chaperone proteins into cellular compartments, including the nucleus (24, 25).

The presence of NQO1 in the nucleus is of significant interest because of its utility as a target for bioreductively activated antitumor quinones. These agents cause toxicity via direct DNA damage so the presence of NQO1 in the nuclear compartment adjacent to DNA could be of considerable importance to the toxicity caused by these agents. NQO1 has also been implicated in the stabilization of p53 (26), and the presence of nuclear NQO1 may also have implications with respect to p53 function. Interestingly, the relative level of nuclear to cytosolic NQO1 was higher in H661 cells, compared with HT29 cells, where a much smaller fraction of NQO1 was present in the nucleus (Figs. 1 and 2), but the mechanisms underlying such differences are currently unclear. The presence of a nuclear compartment of NQO1 may contribute to the lack of correlation that is sometimes observed between the cytotoxicity of antitumor quinones bioactivated by NQO1 and total cellular NQO1 activity (27, 28). In conclusion, we report the presence of significant levels of NQO1 in the nucleus of HT29 colon carcinoma cells and H661 non-small cell lung cancer cells as determined by confocal, immunoelectron microscopy, and cell fractionation techniques. This pool of enzyme may become important in understanding the protective role of NQO1 in cells, as well as the role of NQO1 in the bioactivation of DNA-damaging antitumor agents.

REFERENCES

1. Ernster, L. DT-diaphorase. Methods Enzymol., *10:* 309–317, 1967.
2. Ross, D. Quinone Reductases. *In*: F. P. Guengerich, I. G. Sipes, C. A. McQueen, and A. J. Gandolfi (eds.), Comprehensive Toxicology, Vol. 3, pp. 179–197. Elsevier, 1997.
3. Beyer, R. E., Segura-Aguilar, J., Di Bernardo, S., Cavazzoni, M., Fato, R., Fiorentini, D., Galli, M. C., Setti, M., Landi, L., and Lenaz, G. The role of DT-diaphorase in the maintenance of the reduced antioxidant form of coenzyme Q in membrane systems. Proc. Natl. Acad. Sci. USA, *93:* 2528–2532, 1996.
4. Landi, L., Fiorentini, D., Galli, M. C., Segura-Aguilar, J., and Beyer, R. E. DT-Diaphorase maintains the reduced state of ubiquinones in lipid vesicles thereby promoting their antioxidant function. Free Radic. Biol. Med., *22:* 329–335, 1997.
5. Siegel, D., Bolton, E. M., Burr, J. A., Liebler, D. C., and Ross, D. The reduction of α-tocopherolquinone by human NAD(P)H: quinone oxidoreductase: the role of α-tocopherolhydroquinone as a cellular antioxidant. Mol. Pharmacol., *52:* 300–305, 1997.
6. Ross, D., Siegel, D., Beall, H., Prakash, A. S., Mulcahy, R. T., and Gibson, N. W. DT-diaphorase in activation and detoxification of quinones. Bioreductive activation of mitomycin C. Cancer Metastasis Rev., *12:* 83–101, 1993.
7. Ross, D., Beall, H., Traver, R. D., Siegel, D., Phillips, R. M., and Gibson, N. W. Bioactivation of quinones by DT-diaphorase, molecular, biochemical, and chemical studies. Oncol. Res., *6:* 493–500, 1994.
8. Kelsey, K. T., Ross, D., Traver, R. D., Christiani, D. C., Zuo, Z. F., Spitz, M. R., Wang, M., Xu, X., Lee, B. K., Schwartz, B. S., and Wiencke, J. K. Ethnic variation in the prevalence of a common NAD(P)H quinone oxidoreductase polymorphism and its implications for anti-cancer chemotherapy. Br. J. Cancer, *76:* 852–854, 1997.
9. Siegel., D., Anwar, A., Winski, S. L., Kepa, J. K., Dowd, K. L., and Ross, D. Rapid polyubiquitination and proteasomal degradation of a mutant form of NAD(P)H: quinone oxidoreductase 1. Mol. Pharmacol., *59:* 263–268, 2001.
10. Rothman, N., Smith, M. T., Hayes, R. B., Traver, R. D., Hoener, B., Campleman, S., Li, G. L., Dosemeci, M., Linet, M., Zhang, L., Xi, L., Wacholder, S., Lu, W., Meyer, K. B., Titenko-Holland, N., Stewart, J. T., Yin, S., and Ross, D. Benzene poisoning, a risk factor for hematological malignancy, is associated with the NQO1 609C–>T mutation and rapid fractional excretion of chlorzoxazone. Cancer Res., *57:* 2839–2842, 1997.
11. Larson, R. A., Wang, Y., Banerjee, M., Wiemels, J., Hartford, C., Le Beau, M. M., and Smith, M. T. Prevalence of the inactivating 609C–>T polymorphism in the NAD(P)H:quinone oxidoreductase (NQO1) gene in patients with primary and therapy-related myeloid leukemia. Blood, *94:* 803–807, 1999.
12. Smith, M. T., Wang, Y., Kane, E., Rollinson, S., Wiemels, J. L., Roman, E., Roddam, P., Cartwright, R., and Morgan, G. Low NAD(P)H. quinone oxidoreductase 1 activity is associated with increased risk of acute leukemia in adults. Blood, *97:* 1422–1426, 2001.
13. Clairmont, A., Sies, H., Ramachandran, S., Lear, J. T., Smith, A. G., Bowers, B., Jones, P. W., Fryer, A. A., and Strange, R. C. Association of NAD(P)H:quinone oxidoreductase (NQO1) null with numbers of basal cell carcinomas: use of a multivariate model to rank the relative importance of this polymorphism and those at other relevant loci. Carcinogenesis (Lond.), *20:* 1235–1240, 1999.
14. Cresteil, T., and Jaiswal, A. K. High levels of expression of the NAD(P)H:quinone oxidoreductase (NQO1) gene in tumor cells compared to normal cells of the same origin. Biochem. Pharmacol., *42:* 1021–1027, 1991.
15. Schlager, J. J., and Powis, G. Cytosolic NAD(P)H. (quinone-acceptor)oxidoreductase in human normal and tumor tissue: effects of cigarette smoking and alcohol. Int. J. Cancer, *45:* 403–409, 1990.
16. Malkinson, A. M., Siegel, D., Forrest, G. L., Gazdar, A. F., Oie, H. K., Chan, D. C., Bunn, P. A., Mabry, M., Dykes, D. J., Harrison, S. D., and Ross, D. Elevated DT-diaphorase activity and messenger RNA content in human non-small cell lung carcinoma: relationship to the response of lung tumor xenografts to mitomycin Cl. Cancer Res., *52:* 4752–4757, 1992.
17. Benson, A. M., Hunkeler, M. J., and Talalay, P. Increase of NAD(P)H:quinone reductase by dietary antioxidants: possible role in protection against carcinogenesis and toxicity. Proc. Natl. Acad. Sci. USA, *77:* 5216–5220, 1980.

18. McDonald, K. L. Electron microscopy and EM immunocytochemistry. Methods Cell Biol., *44:* 411–444, 1994.
19. Conover, T. E., and Ernster, L. DT Diaphorase: relation to respiratory chain of intact mitochondria. Biochim. Biophys. Acta, *58:* 189–200, 1962.
20. Edlund, C., Elhammer, A., and Dallner, G. Distribution of newly synthesized DT-diaphorase in rat liver. Biosci. Rep., *2:* 861–865, 1982.
21. Eliasson, M., Bostrom, M., and DePierre, J. W. Levels and subcellular distributions of detoxifying enzymes in the ovarian corpus luteum of the pregnant and non-pregnant pig. Biochem. Pharmacol., *58:* 1287–1292, 1999.
22. Segura-Aguilar, J., Cremades, A., Llombart-Bosch, A., Monsalve, E., Ernster, L., and Romero, F. J. Activity and immunohistochemistry of DT-diaphorase in hamster and human kidney tumours. Carcinogenesis (Lond.), *15:* 1631–1636, 1994.
23. Yoneda, Y., Hieda, M., Nagoshi, E., and Miyamoto, Y. Nucleocytoplasmic protein transport and recycling of Ran. Cell Struct. Funct., *24:* 425–433, 1999.
24. Fujihara, S. M., and Nadler, S. G. Intranuclear targeted delivery of functional NF-κB by 70 kDa heat shock protein. EMBO J., *18:* 411–419, 1999.
25. Agostini, I., Popov, S., Li, J., Dubrovsky, L., Hao, T., and Bukrinsky, M. Heat-shock protein 70 can replace viral protein R of HIV-1 during nuclear import of the viral preintegration complex. Exp. Cell Res., *259:* 398–403, 2000.
26. Asher, G., Lotem, J., Cohen, B., Sachs, L., and Shaul, Y. Regulation of p53 stability and p53-dependent apoptosis by NADH quinone oxidoreductase 1. Proc. Natl. Acad. Sci. USA, *98:* 1188–1193, 2001.
27. Mikami, K., Naito, M., Tomida, A., Yamada, M., Sirakusa, T., and Tsuruo, T. DT-diaphorase as a critical determinant of sensitivity to mitomycin C in human colon and gastric carcinoma cell lines. Cancer Res., *56:* 2823–2826, 1996.
28. Winski, S. L., Swann, E., Hargreaves, R. H., Dehn, D. L., Butler, J., Moody, C. J., and Ross, D. Relationship between NAD(P)H:quinone oxidoreductase 1 (NQO1) levels in a series of stably transfected cell lines and susceptibility to antitumor quinones. Biochem. Pharmacol., *61:* 1509–1516, 2001.

Subcellular Localization of NAD(P)H:quinone Oxidoreductase 1 in Human Cancer Cells

Shannon L. Winski, Yiannis Koutalos, David L. Bentley, et al.

Cancer Res 2002;62:1420-1424.